G1-OR-11

Shish-kebab formation process observation using new SANS spectrometer, TAIKAN.

Go Matsuba1*, Masayuki Sakurai1, Taiki Tominaga2, and Shin-ichi Takata2

1.Graduate School of Science and Engineering, Yamagata University, 992-8510 JAPAN

2.J-PARC Center, Japan Atomic Energy Agency, 319-1195 JAPAN

*gmatsuba@yz.yamagata-u.ac.jp

Abstract: We carried out in very precise analysis of the shish and kebab structure based on small and wide angle neutron scattering (SANS and WANS) data with the TAIKAN spectrometer in J-PARC, JAEA, Tokai, Japan. We performed neutron scattering measurements in a wide range of scattering vector $Q = 4\pi/\sin\theta$ (1×10^{-3}~ 2 $Å^{-1}$) on elongated PE blend of low molecular weight deuterated PE (dPE, 97 wt%) and high molecular weight hydrogenated PE (hPE, 3 wt%). We observed the quenched sample in the strain = 0.0, 0.1, 0.4, 1.2, 1.9 and 5.0. In low strain condition (strain = 0.07), the profile was isotropic, and so the effect of strain was not large then the lamellar crystals could not be oriented or broken. After yield point (strain = 0.6), the SANS profiles became anisotropic. The lamellar crystals were oriented stretched direction and the nm scaled shish-structure was grown. On further stretch, we observed 4-point scattering patterns. The lamellar crystals was tilted but the chains was parallel to the stretch direction.

Keywords: Shish-kebab structure; Neutron scattering, Stress-Strain curve

1. Introduction

When polymer are crystallized under uniaxial draw, shear flows or mixed flows, the so-called shish-kebab structure could be observed. Pennings et al. found this special morphology in stirring of the polyethylene solution [1]. The shish-kebabs consist of long central fiber core (shish) and lamellar crystal (kebab) periodically attached along the shish-structure. It is believed that the shish-kebab structure is one of origins of ultra high strength and ultra high modulus of fibers/plastics, and hence intensive studies have been performed by many research groups. For example, Keller et al. observed shish-kebab structure in polyethylene (PE) using transmission electron microscope (TEM) and found that the shish was about 10 nm in diameter and several microns in height [2-4]. On the other hands, long oriented objects with diameters of several μm were observed during shear-induced crystallization of some polymers [5-8]. These long oriented objects in μm scale are similar to the shish-structure apparently, but the size is completely different. These observations suggest that the shish-kebab structure has hierarchical structure in a wide spatial scale. However, the structural formation process of shish-kebabs is not fully understood, because the amount of kebabs is much larger than that of shishs especially for small angle X-ray scattering (SAXS) technique.

We succeeded the shish formation process. Especially, we focused on the shish-kebab formation process during uniaxial draw with in-situ small angle neutron scattering (SANS) and SAXS measurements. The SAXS and SANS profiles were analyzed to clarify the mechanism of structure development from isotropic lamella crystals to the shish-kebab structure. In the early stage of draw, the long spacing period increased and crystal growth was induced by elongation. Then, the spot-like scattering profiles in the parallel direction of elongation were observed due to the kebab structure. On further drawing, both the spot-like scattering profiles in parallel and streak-like scattering in normal direction of drawing were observed. The developments of shish structure occurred in the very early stage of draw from SANS precise analysis because the intensity especially increases very significantly with increasing draw ratio. We insisted that the chains might be pulled out from the lamellae, disentangled and oriented along the drawing direction [9].

Furthermore, we performed neutron and x-ray scattering measurements in a wide range of scattering vector $Q = 4\pi/\sin\theta$ (1 x 10^{-4}~ 3 $Å^{-1}$), where 2θ is the scattering angle, on elongated PE blend of low molecular weight deuterated PE (dPE) and high molecular weight hydrogenated PE (hPE). We found that the large oriented and aligned objects were formed from the high molecular weight hPE. Analyzing the data quantitatively in terms of the multi-core shell cylinder model we also found that the large oriented structure in μm scale was about 1 μm in radius and about 6 μm in height, and included about three extended chain crystals with radius of about 4.5 nm [10].

In order to clarify the correlation between structure formation and stress-strain curve during uniaxial drawing, we carried out in very precise analysis of the shish and kebab structure based on small and wide angle neutron scattering (SANS and WANS) data with the TAIKAN spectrometer in J-PARC, JAEA, Tokai, Japan.

2. Experimentals

2.1 Samples

We used high molecular weight hPE (M_w = 2,000,000 and M_w/M_n = 12) and dPE (M_w = 600,000, M_w/M_n = 2) through this experiment. The nominal melting temperatures of hPE and dPE determined by DSC measurements were 132 ˚C and 128 ˚C at a heating rate of 5 °C/min, respectively. The blends of hPE and dPE were dissolved in hot *o*-dichlorobenzene with antioxidant reagent (2,6-*t*-butyl-*p*-cresole) to form a homogeneous solution and poured into methanol. After vacuum-drying at room temperature for several days the blended samples were hot-pressed at 170 ˚C with a thickness of about 0.5 mm. The concentration of hPE in the blend was 3 wt %.

2.2 Drawing

Uniaxial drawing of the films was performed at 125 °C with a Compact tensile and compression tester (IMC-18E0, Imoto Machinery, Kyoto, Japan). The strain rate was 5 mm/s. Figure 1 shows the stress-strain curve for one of measurement samples. The yield point of these samples was 0.6 and elongation at break was 7 at least. We observed the quenched sample in the

strain = 0.0, 0.07, 0.6 (Yield Point), 1.2, 2.8 and 5.0.

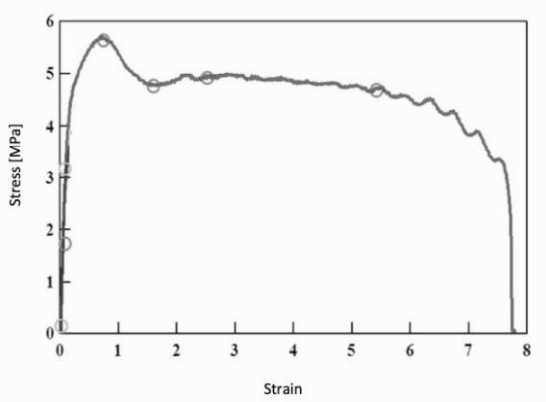

Figure 1 Stress-Strain curve for polyethylene blended samples

2.3 Apparatus

2.3.1 SAXS Measurements

Simultaneous small-angle and wide-angle x-ray scattering (SAXS/WAXS) measurements were carried out at the beam-line BL-6A, Photon Factory, KEK, Tsukuba, Japan. The camera length was 2.1 m and 75 mm for SAXS and WAXS, respectively, and x-ray wavelength was 1.5 Å. A CCD camera (C7330) for SAXS with an image intensifier and a plat panel CCD camera (C9252DK-14) for WAXS (Hamamatsu Photonics K.K.) were used as a detector system [11,12]. The Q range was 8 x 10^{-3} and 0.15 $Å^{-1}$ for SAXS and 0.5 and 2.5 $Å^{-1}$ for WAXS. The exposure time was 0.5 s for SAXS/WAXS measurements.

2.3.2 SANS Measurements

The small and wide angle neutron scattering instrument, TAIKAN, was installed on BL15 in the Materials and Life Science Experimental Facility (MLF) of J-PARC, Tokai, Japan. TAIKAN is designed for efficient measurement in wide-Q range of 0.005 ~ 20 $Å^{-1}$ with time-of-flight neutron scattering methods. The 1040 3He-PSD tubes with 8 mm in diameter and gas pressure of 6 atm are mounted on four detector banks of small-, middle-, high-, and backward-angle. The two detector banks in the chamber are surrounded by the B4C shielding boards, in order to avoid the crosstalk between facing detectors and reduce the background [13].

3. Results and Discussion

3.1 2D SAXS and WAXS Profiles

Figure 2 shows 2D SAXS and WAXS profiles for various strain conditions. The SAXS and WAXS patterns before drawing are isotropic and show a broad scattering maximum at around Q = 0.02 $Å^{-1}$. The peak is assigned to the long period. The lamellae are distributed isotropically in the sample crystallized at 125 °C. In low strain condition (strain = 0.07), the profile was isotropic, and so the effect of strain was not large then the lamellar crystals could not be oriented or broken. After yield point (strain = 0.6), lamellar crystals as well as crystal lattice began to orient along the drawing direction. The lamellar crystals were oriented stretched direction. From WAXS measurements, we observed the so-called fiber pattern that is strongly oriented crystal lattice. On further stretch above strain = 2.8, we observed 4-point scattering patterns. The lamellar crystals were tilted but the chains were parallel to the stretch direction [14]. Then the scattering profiles became weaker during drawing process at strain = 5.0 because the sample film became thinner during drawing process. On the other hands, the shish-structure could not be observed with SAXS measurements because the amount of

shish-structure is too small. These phenomena are consistent of our previous results [9,10].

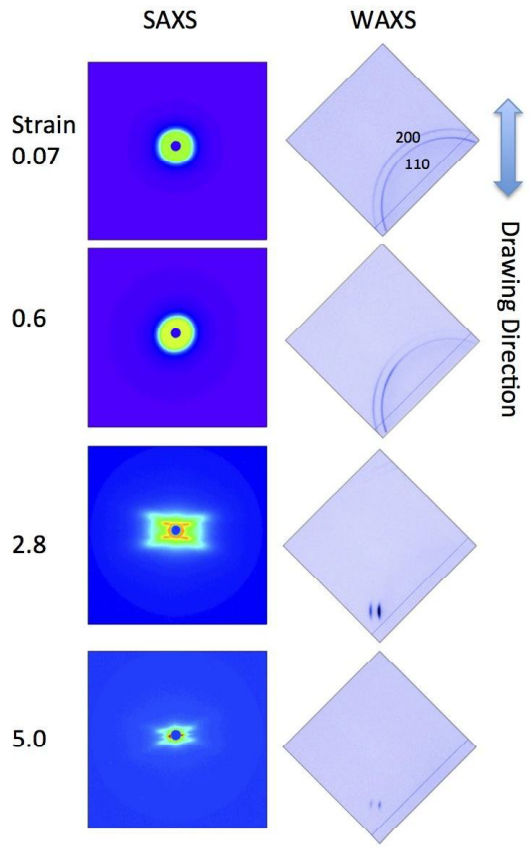

Figure 2 2D SAXS (Left) and WAXS (Right) profiles in various strains.

3.2 2D SANS Profiles

Figure 3 shows the 2D SANS profiles for various strain conditions. At first, before drawing, the SANS profile was isotropic. After the yield point, the SANS profiles became anisotropic. Below strain = 2.8, the SANS profiles is quite similar as the SAXS ones, because the SANS intensity was caused by the density fluctuation between lamellar crystals and inter-lamellar amorphous region. After further stretching, we observed both 4-point scattering patterns and strong streak-like scattering normal to the drawing direction. The streak-like scattering is assigned as the shish-structure and/or micron-scale cylinder-type structure from our previous results. These results suggest the lamellae begin to be tilted induced by draw process and chains are pulled out and disentangled from lamellae, then the chains was parallel to the stretch direction then absorbed into the shish-structure [14].

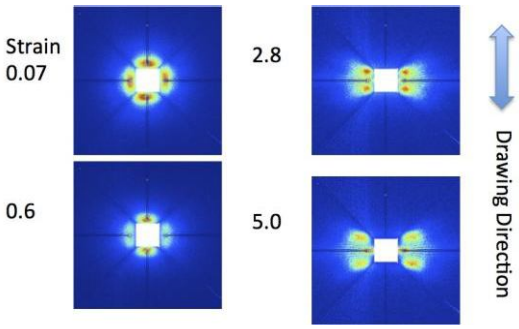

Figure 3 2D SANS profiles in various strains.

In order to evaluate the shish formation, we calculated the 1D SANS profiles in the normal direction in Figure 4. In the low strain, streak-like scattering profiles were not so clear in Figure 3; we could observe only the isotropic lamellar structure. As the strain increase, the SANS intensity decreases with draw ratio in Q = 0.02 $Å^{-1}$. The peak around Q = 0.02 $Å^{-1}$ is assigned to the long spacing period of isotropic lamella, then the long spacing period is about 300 Å (=$2\pi/Q$). One possibility of the reducing around Q = 0.02 $Å^{-1}$ is rotation and orientation of the isotropic crystal lamella during drawing. It is noted that the intensity especially above Q = 0.06 $Å^{-1}$ increases significantly with increasing draw ratio. The results mean that the formation of the nm-scale shish structure consisting of high molecular weight hPE has already occurred at the yield point. After the yield point, 10 nm scaled shish-structure starts to grow.

For detailed analysis of nm scaled structure,

Figure 5 shows the SANS intensity of normal direction to the drawing in a very wide *Q*-range from 0.02 to 2.0 Å^{-1}. The peaks at Q = 1.5 and 1.72 Å^{-1} are the diffraction of (110) and (200), respectively. The intensity increases with drawing process. The hPE component could be oriented after drawing comparing to dPE components.

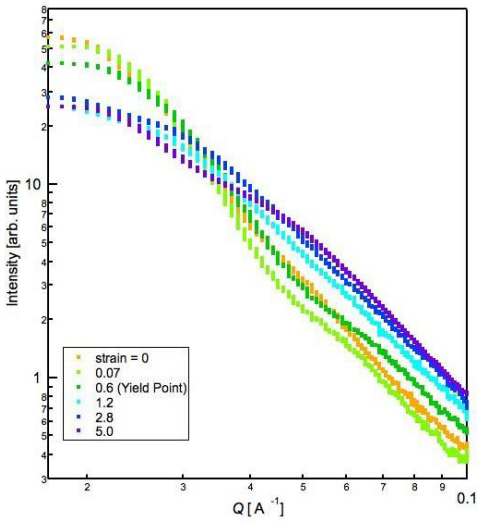

Figure 4 SANS profiles in normal direction of elongation in various strains.

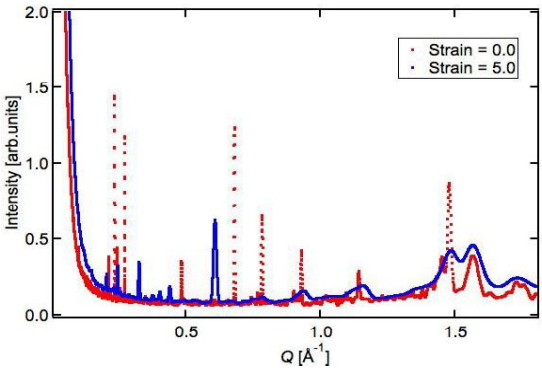

Figure 5 SANS profiles of wide Q range in normal direction of elongation for before drawing (Strain = 0.0) and after drawing (5.0).

4. Conclusion

We have studied the development of shish-kebab structure of a blend of dPE (97 wt%) and high molecular weight hPE (3 wt%) during uniaxial drawing process by means of SAXS and SANS techniques. In order to discuss about wide spatial scale structure and correlation of high molecular weight components, time-of-flight neutron scattering measurements were carried out at a new spectrometer, TAIKAN, at J-PARC. In low strain, the intensity of long spacing period decreases with drawing process. At the yield point, the 10 nm scaled shish developments occurred from SANS precise analysis because the intensity especially above Q = 0.04 Å^{-1} increases very significantly with increasing strain. On further drawing, the spot-like scattering patterns became to 4-point scattering patterns. We insisted that the lamellar crystals were tilted but the chains were parallel to the stretch direction.

4. Acknowledgments

These SAXS works have been performed under the approval of the Photon Factory Program Advisory Committee (Proposal No. 2012G025, 2012G525). The TOF-SANS experiments were carried out under the approval of CROSS (Proposal No.2012A0019).

References

[1] A. J. Pennings, A. M. Kiel, Kolloid Z. Z. Polym., 1965, 205: 160-162.

[2] J. A. Odell, D. T. Grubb, A. Keller, Polymer, 1978, 19: 617-626.

[3] Z. Bashir, J. A. Odell, A. Keller, J. Mater. Sci., 1984, 19: 3713-3725.

[4] Z. Bashir, M. J. Hill, A. Keller, J. Mater. Sci. Lett., 1986, 5: 876-878.

[5] H. Fukushima, Y. Ogino, G. Matsuba, K. Nishida, T. Kanaya, Polymer, 2005, 46(6): 1878-1885.

[6] G. Matsuba, S. Sakamoto, Y. Ogino, K. Nishida, T. Kanaya, Macromolecules, 2007, 40(20): 7270-7275.

[7] Y. Hayashi, G, Matsuba, Y. Zhao, K. Nishida, T. Kanaya,. Polymer, 2009, 50: 2095-2103.

[8] Y. Zhao, G, Matsuba, K. Nishida, T. Fujiwara, R. Inoue, I. Polec, C. Deng, T. Kanaya, J. Polym. Sci. Part B: Polym. Phys., 2011, 49(3): 214-211.

[9] G. Matsuba, C. Ito, Y. Zhao, R. Inoue, K. Nishida, T. Kanaya, Polym. J., 2013, 45(3): 293-299.

[10] T. Kanaya, G. Matsuba, Y. Ogino, K. Nishida, H. M. Shimizu, T. Shinohara, T. Oku, J. Suzuki, T. Otomo, Macromolecules, 2007, 40: 3650-3657.

[11] Y. Amemiya, K. Wakabayashi, T. Hamanaka, T. Wakabayashi, H. Hashizume., Nucl. Instr. Meth., 1983, 208, 471-477.

[12] N. Igarashi, Y. Watanabe, Y. Shinohara, Y. Inoko, G. Matsuba, H. Okuda, T. Mori and K. Ito, J. Phys: Conf. Series, 2011, 272(1): 012026.

[13] T. Shinohara, S. Takata, J. Suzuki, K. Suzuya, K. Aizawa, M. Arai, T. Otomo, M. Sugiyama, Nucl. Instr. Meth., 2009, 800(1): 111-113.

[14] W. Wang, N.S. Murthy, D.T. Grubb, Polymer, 2007, 48(12): 3393-3399.